

Supporting information

Molecular Materials through Microdroplets: Synthesis of Protein-Protected Luminescent Clusters of Noble Metals

Sandeep Bose,¹ Amit Chatterjee,² Shantha Kumar Jenifer,¹ Biswajit Mondal,¹ Pillalamarri Srikrishnarka,¹ Debasmita Ghosh,¹ Angshuman Ray Chowdhuri,¹ M. P. Kannan,¹ Sailaja V. Elchuri,² Thalappil Pradeep^{1,*}

¹DST Unit of Nanoscience (DST UNS) and Thematic Unit of Excellence (TUE), Department of Chemistry, Indian Institute of Technology Madras, Chennai - 600 036, India

²Department of Nanobiotechnology, Vision Research Foundation, Sankara Nethralaya, Chennai-600006, India

*Email: pradeep@iitm.ac.in

SUPPORTING INFORMATION CONTENT

Total number of pages – 16

Total number of figures – 19

Total number of tables – 0

Figures	Table of Contents	Page no.
	Instrumentation	S2
Figure S1	Comparison of the luminescence of clusters synthesized at two different electrospray potentials	S4
Figure S2	Comparison of the PL spectra of the sample obtained with and without using electrospray after 1 h	S5
Figure S3	TEM image of the Au and Ag nanoparticles obtained after spray in absence of electric field	S6
Figure S4	UV-Vis spectra of Au and Ag nanoparticles obtained as result of spray in the absence of electric field	S6

Figure S5	Comparison of UV-Vis spectrum of Au ₃₀ @BSA synthesized by both the SP and ES method	S7
Figure S6	Absorption and luminescence spectra of ES Au@Lyz and ES Ag@BSA	S7
Figure S7	XPS spectra of Au and Ag in ES Au@Lyz and ES Ag@BSA	S8
Figure S8	XPS spectra of Sulphur present in the ES Au@BSA, ES Ag@BSA and ES Au@Lyz clusters	S9
Figure S9	TEM images of ES Ag@BSA and ES Au@Lyz	S10
Figure S10	UV-Vis and TEM features of all the SP clusters	S10
Figure S11	Time-dependent stability and effect of pH on the luminescence of ES cluster	S11
Figure S12	Distance-dependent changes in the luminescence intensity of ES Au@BSA	S11
Figure S13	High-speed camera images of the charged microdroplets	S12
Figure S14	Speed of the individual droplets against droplet number for all the ES clusters	S13
Figure S15	Comparison of quantum yields of SP and ES clusters	S14
Figure S16	Comparison of infrared spectra of only BSA and ES Au@BSA cluster	S14
Figure S17	Stability of the cluster in the RPMI 1640 medium and excitation and emission spectra of ES Au@BSA cluster	S15
Figure S18	Fluorescence image of the cells incubated with ES Au@BSA cluster after 1 h	S15
Figure S19	Photo-bleaching experiments performed on the ES Au@BSA cluster and dye (Rhodamine-6G)	S16

Instrumentation

Droplet synthesized clusters were characterized high-resolution transmission electron microscopy (HRTEM), X-ray photoelectron spectroscopy (XPS), photoluminescence (PL) spectroscopy, UV-Vis spectroscopy, fluorescence microscopy, circular dichroism (CD), Fourier-transform infrared spectroscopy (FTIR) and matrix-assisted laser desorption ionization mass spectrometry (MALDI MS). UV-Vis absorption spectra were recorded using a Perkin Elmer Lambda 25 spectrophotometer. Optical absorption spectra were typically measured in the range of 200-1100

nm with a band-pass filter of 1 nm. MALDI MS of the cluster was measured using Voyager-DE Pro Biospectrometry Workstation from Applied Biosystems. TEM measurements were performed using JEOL3010 (JEOL Japan) operating at 200 kV. Photoluminescence measurements were carried out in a HORIBA, Jobin Yvon Nanolog fluorescence spectrometer. Band-pass of 3 nm was used for all the excitation and emission spectra. XPS measurements were conducted with an Omicron ESCA probe spectrometer with polychromatic Mg K α X-rays ($h\nu = 1253.6$ eV). A high-speed camera (Phantom v1212) coupled with Keyence VH-Z100R, zoom lens was used for the measurement of the travel time of droplets. To visualize the electrospray 700 x magnification was set. FTIR was carried out with PerkinElmer spectrum 2 with universal attenuated total reflectance (UATR) with a diamond crystal. Photographic images were taken with a Nikon D5100 DSLR camera. The cells were imaged using a fluorescence microscope (Carl Zeiss, Germany) and image acquisition was performed using a high-NA oil immersion objective of 100X magnification. The sample was excited at 405 and 488 nm. For 405 nm excitation, emission was collected from 410 to 550 nm, and for 488 nm excitation, emission was collected from 520 to 690 nm. For electrospray, the aqueous solution was pushed through a NE-300 infusion syringe pump.

Calculation of the time of travel of the Si QDs at different distances

For calculating the time required to travel from tip of the nozzle to the substrate, the average velocity of about 20 microdroplets coming out of nozzle at different distances were calculated.

For the calculation of time of travel between the tip to substrate the following formula was used:

$$\text{Time (t)} = \text{Total number of frames/frame rate}$$

Once the distance and time were known, the speed of each droplet was calculated by plotting it as a function of the individual droplets. This was fitted with a straight line. After the velocity was

calculated, other parameters were fixed and the distance between the tip to substrate was fixed at 5 mm for each of the cluster. The time required to travel was calculated by the formula, $t = s/v$, where,

t = Average time required by the droplets to reach the substrate.

S = Distance between the tip and substrate

v = Average velocity of the droplet

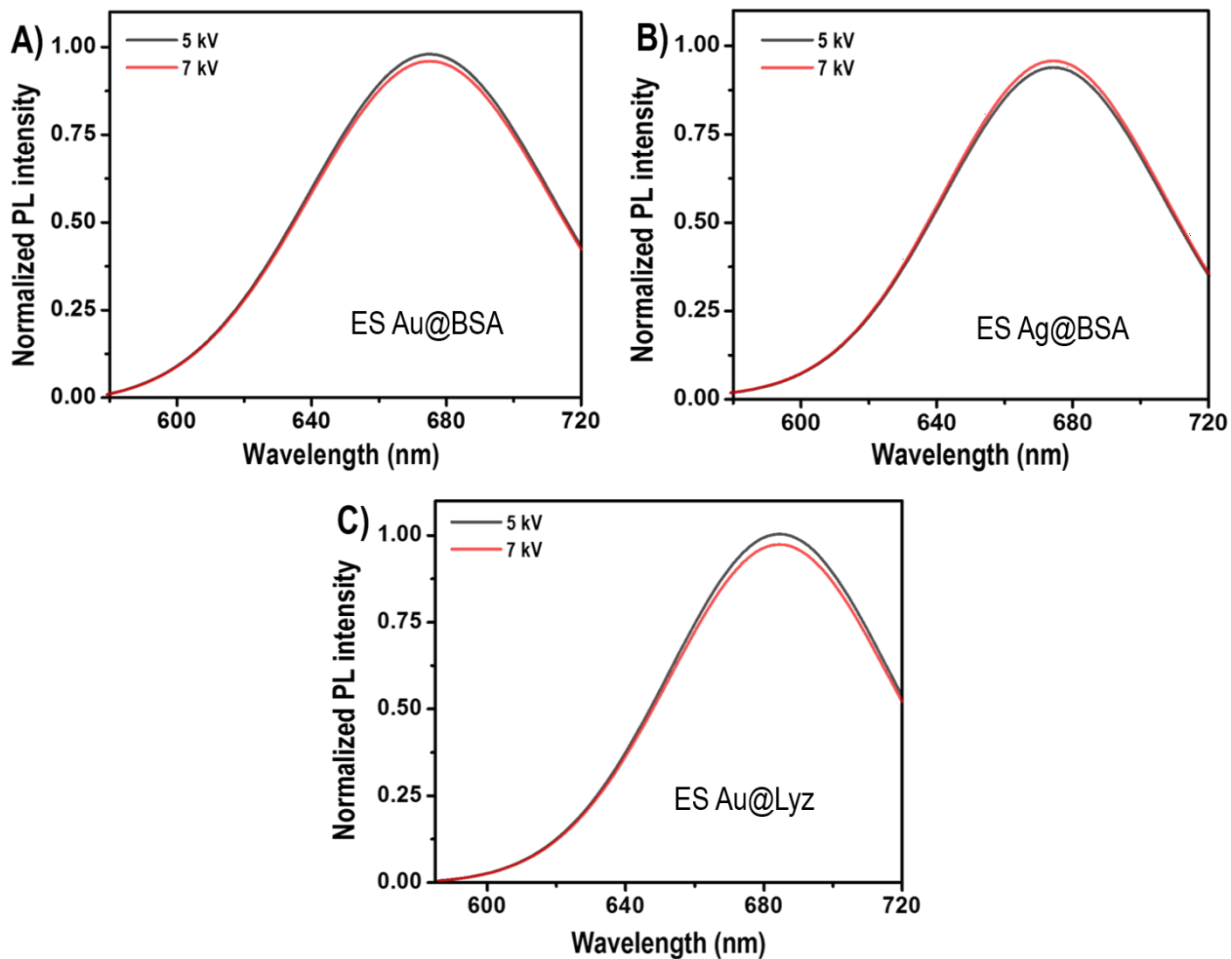


Figure S1. A comparison of the luminescence of clusters synthesized at two different electro spray potentials.

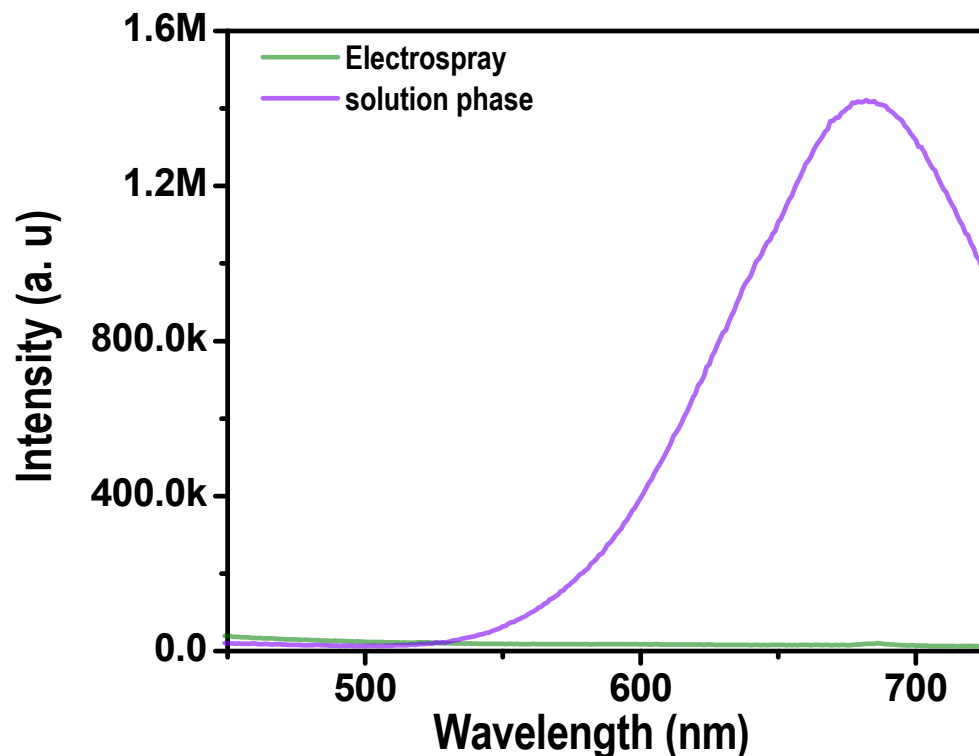


Figure S2. Comparison of PL spectra of the ES and SP sample after 1 h of reaction. After 1 h of electro spray, PL spectrum shows luminescence which suggests that Au@BSA cluster was formed. In order to prove that there was no reaction within 1 h in the solution phase, a mixture of precursors was kept for 1 h and the PL spectrum was measured. No luminescence was observed in the solution phase during this time scale.

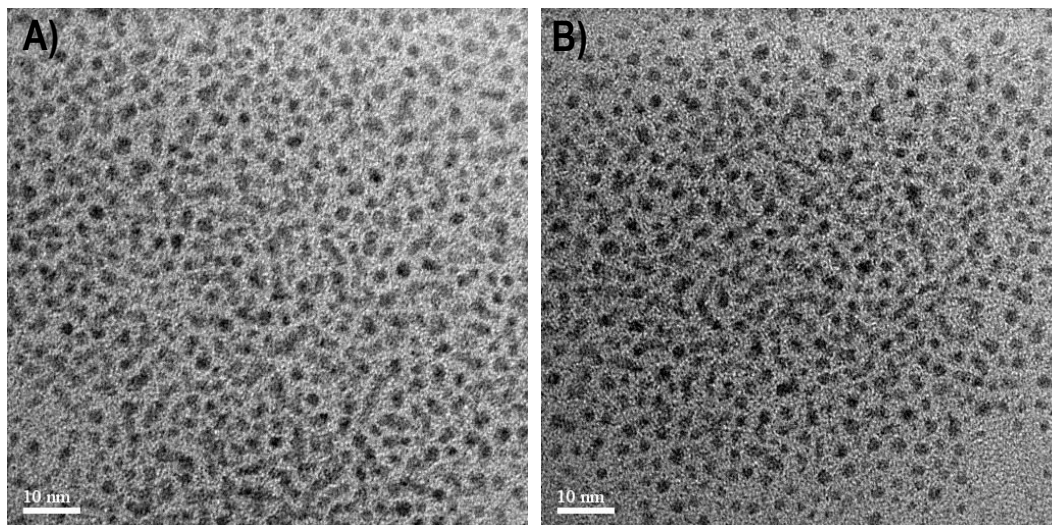


Figure S3. A) TEM image of the Au nanoparticles obtained when the spray was performed using nebulizing gas in the absence of an electric field. B) TEM image of the Ag nanoparticles obtained under similar conditions. See also Figure S3. It produced non-luminescent nanoparticles.

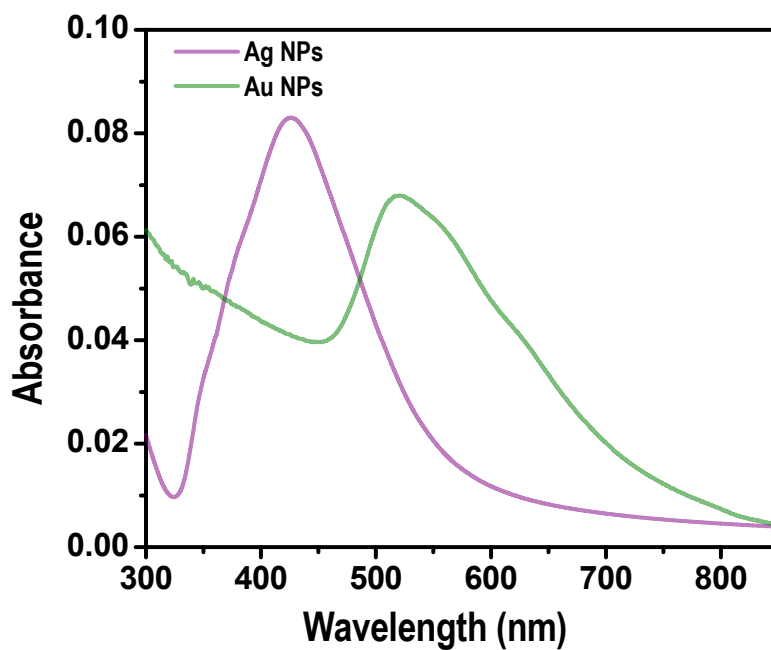


Figure S4. UV-Vis spectra of Ag and Au nanoparticles obtained after spray in the absence of electric field.

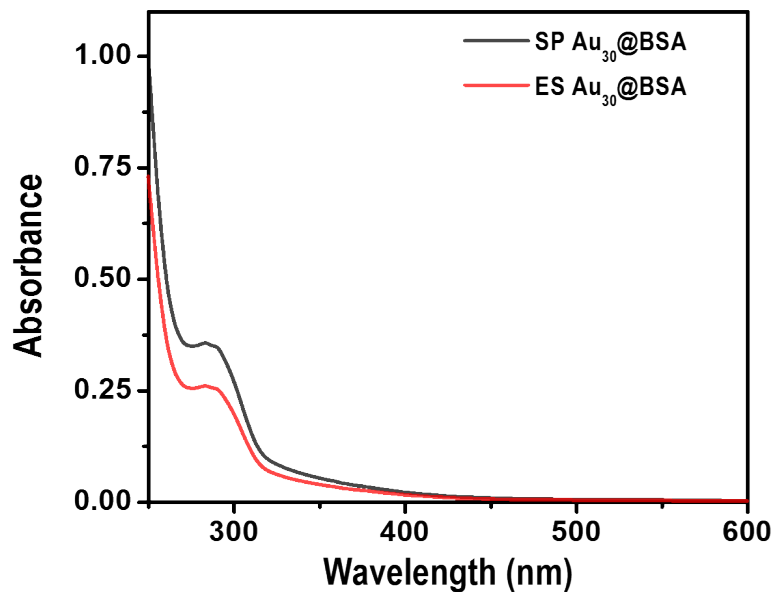


Figure S5. A comparison of UV-Vis spectra of $\text{Au}_{30}\text{@BSA}$ synthesized by the SP and ES methods. $\text{Au}_{30}\text{@BSA}$ synthesized by both these methods show similarities in the UV-Vis spectra.

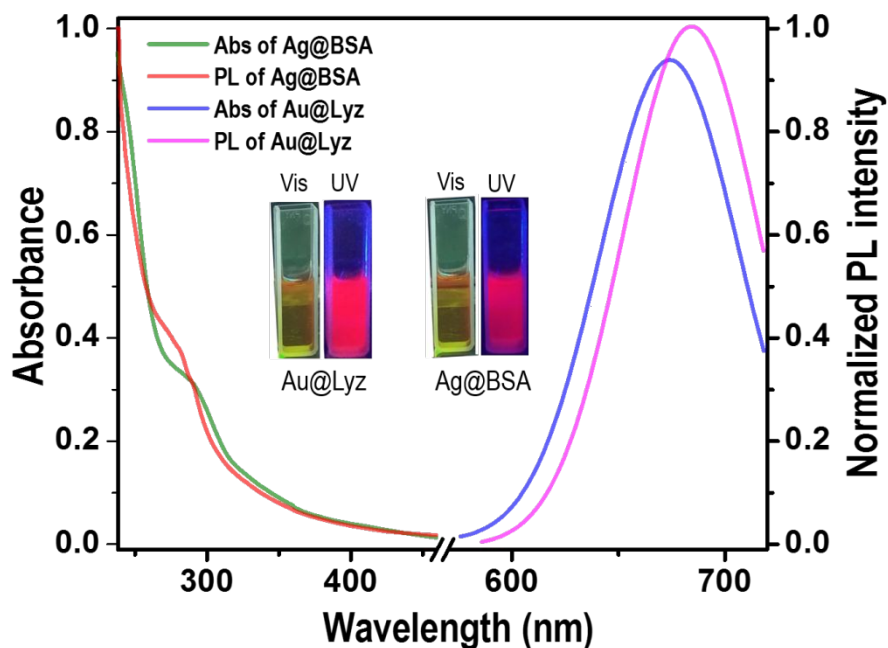


Figure S6. Absorbance (Abs) and photoluminescence (PL) spectra of ES Au@Lyz and ES Ag@BSA obtained as a result electrospay. Inset shows the photographs of ES Au@Lyz and ES Ag@BSA .

Ag@BSA under UV and visible light. Under UV light, both of these clusters show red luminescence.

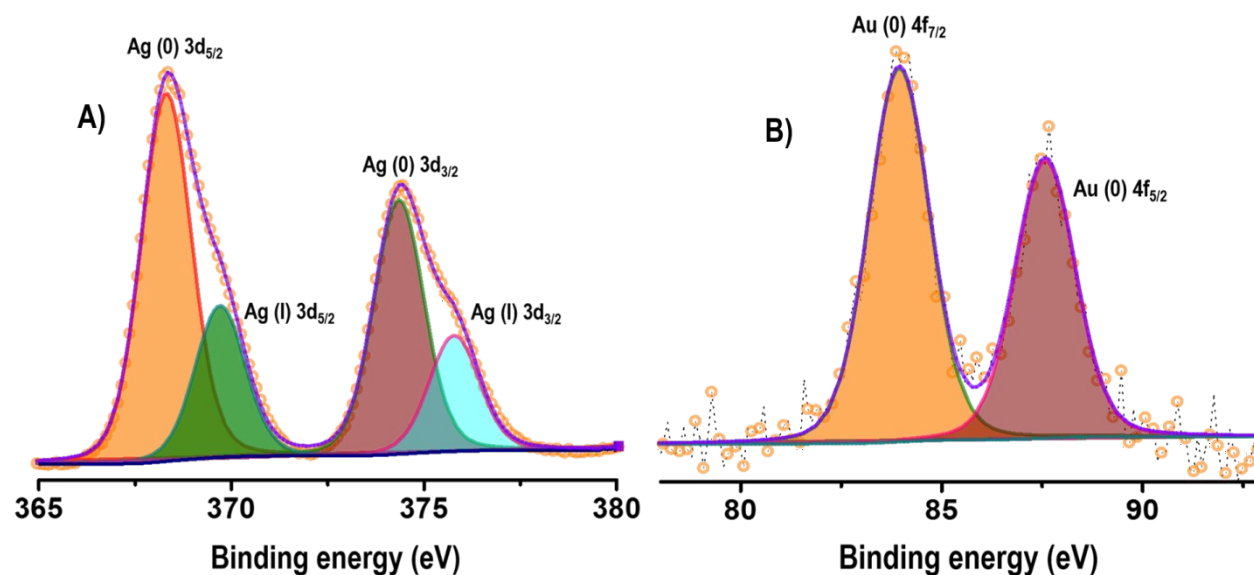


Figure S7. A) and B) are the X-ray photoelectron spectra of ES Ag@BSA and ES Au@Lyz, in the Ag 3d and Au 4f regions, respectively, showing Ag (0) and Au (0) oxidation states in the clusters. The spectrum for Ag (0) shows a higher binding energy component, which is assigned to the positively charged silver atoms bonded to the sulphur atoms of the thiol groups of the protein.

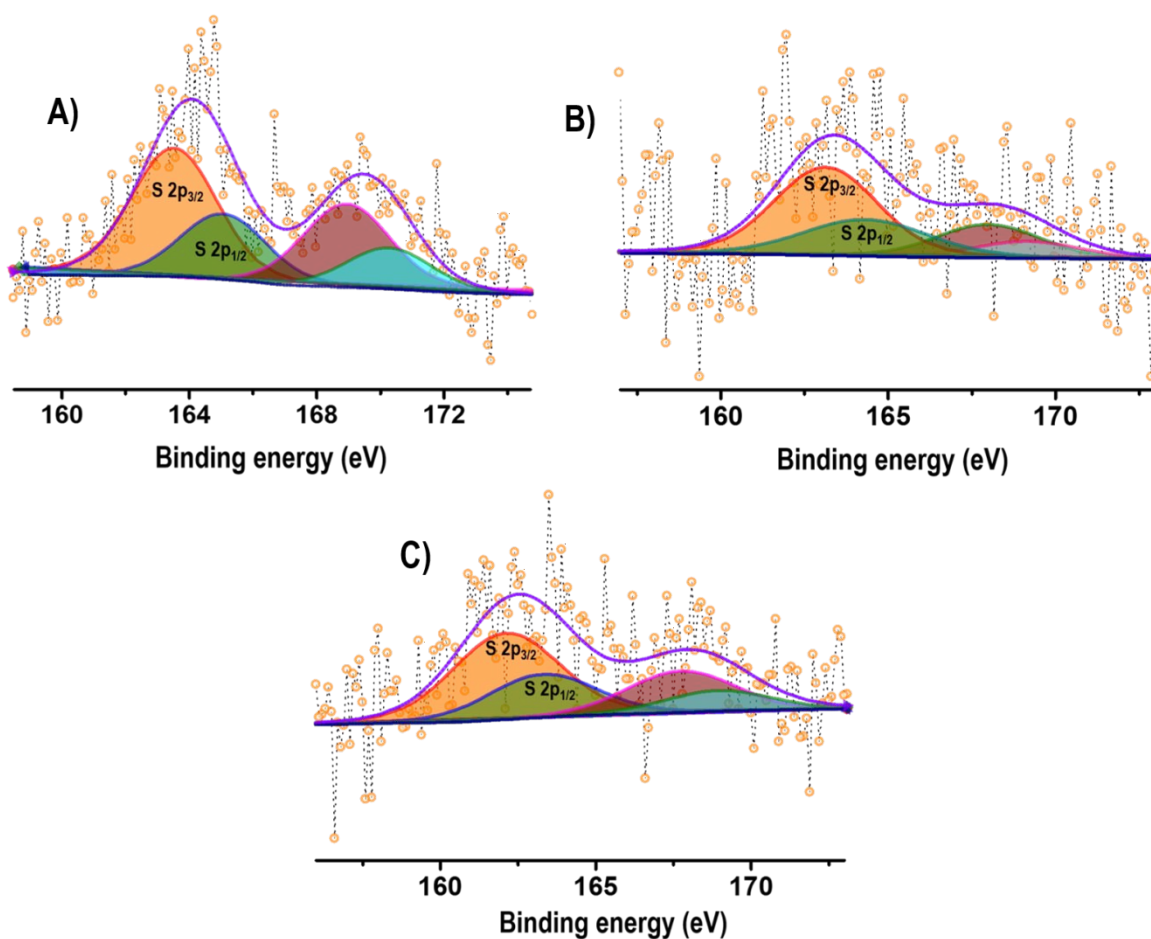


Figure S8. XPS spectra of **A)** ES Au@BSA, **B)** ES Ag@BSA and **C)** ES Au@Lyz, in the S 2p region, showing the oxidized state of sulfur in the clusters. The S 2p_{3/2} feature around 163 eV supports the thiolate binding on the Au/Ag core. Oxidation, contributing to the higher energy features is a characteristic feature in such materials upon X-ray irradiation.

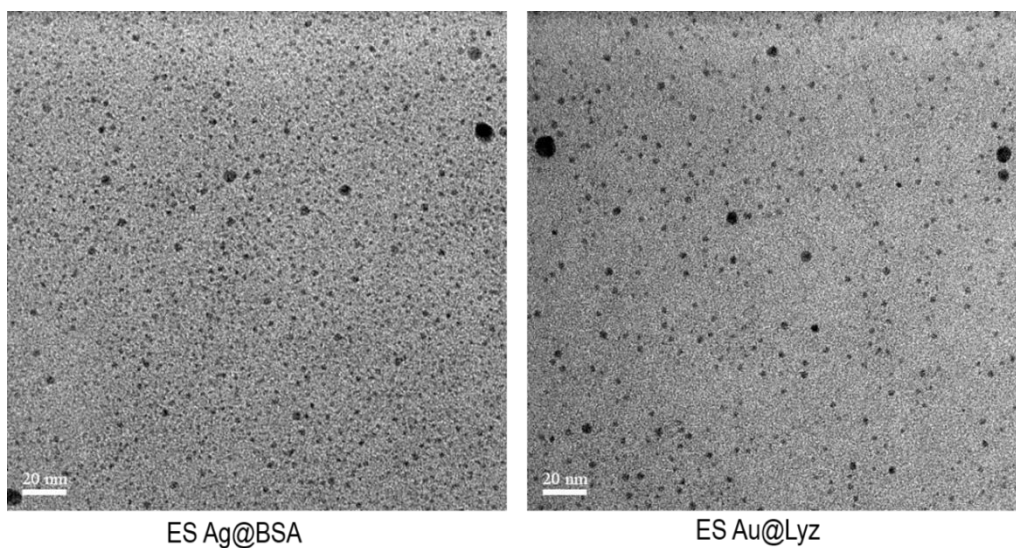


Figure S9. TEM images of ES Ag@BSA and ES Au@Lyz. Electron beam-induced aggregation of clusters is visible.

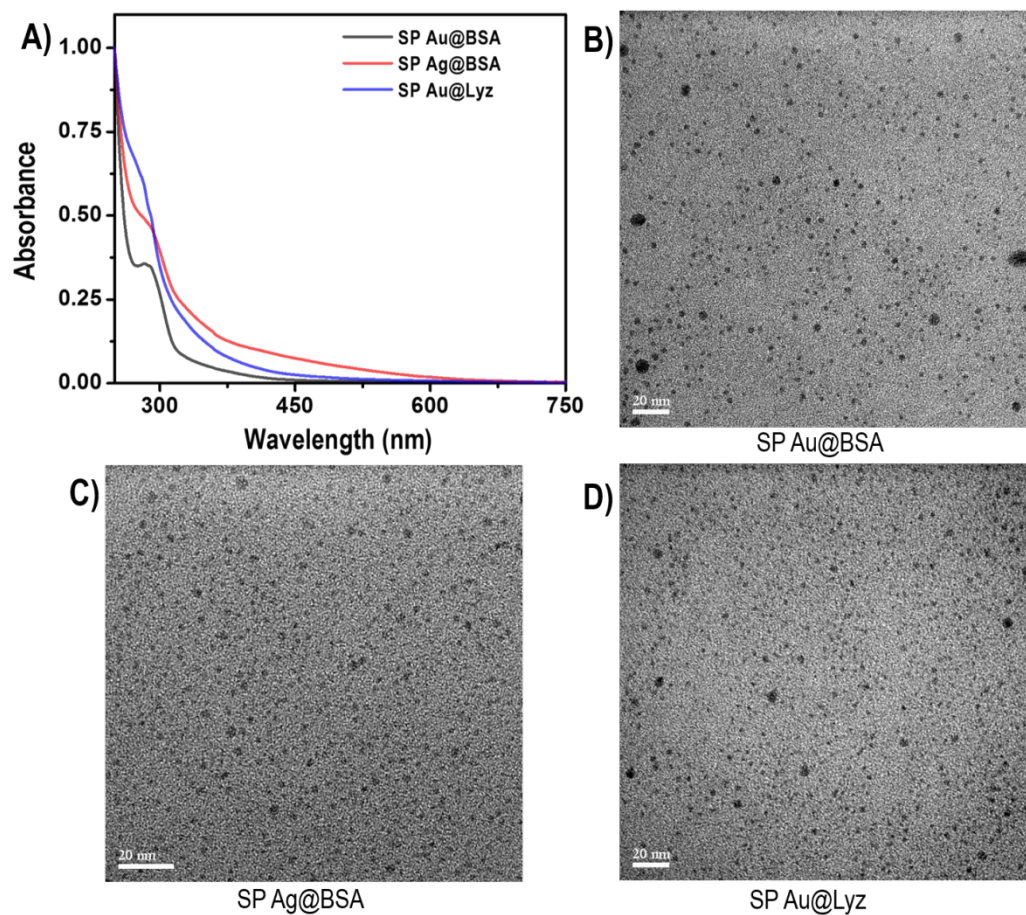


Figure S10. A) UV-Vis feature of all the solution-processed clusters, i.e. SP Au@BSA, SP Ag@BSA and SP Au@Lyz. B), C) and D) are the TEM image of the SP Au@BSA, SP Ag@BSA and SP Au@Lyz, respectively.

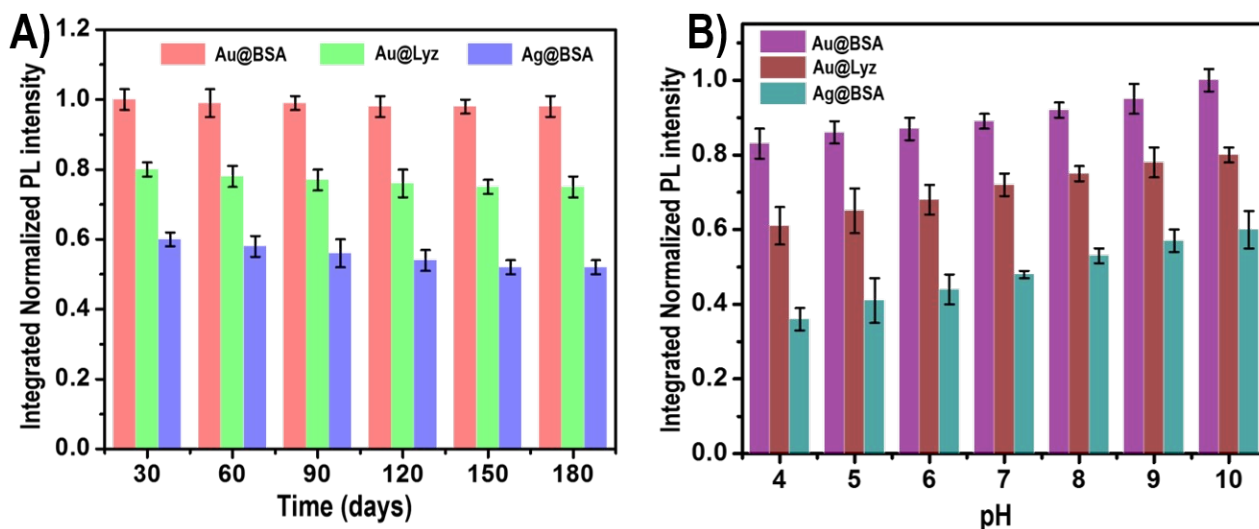


Figure S11. A) Time-dependent stability of the electrospayed clusters measured over a period of six months at an interval of 30 days. Almost no change in the stability was noticed. B) Effect of pH on the luminescence of the electrospayed clusters measured in the range of 4-10. An increase in pH results in the increase in the luminescence. This suggests that unfolding occurs in the alkaline medium due to breakage of disulfide bonds that favors the formation of these luminescent clusters.

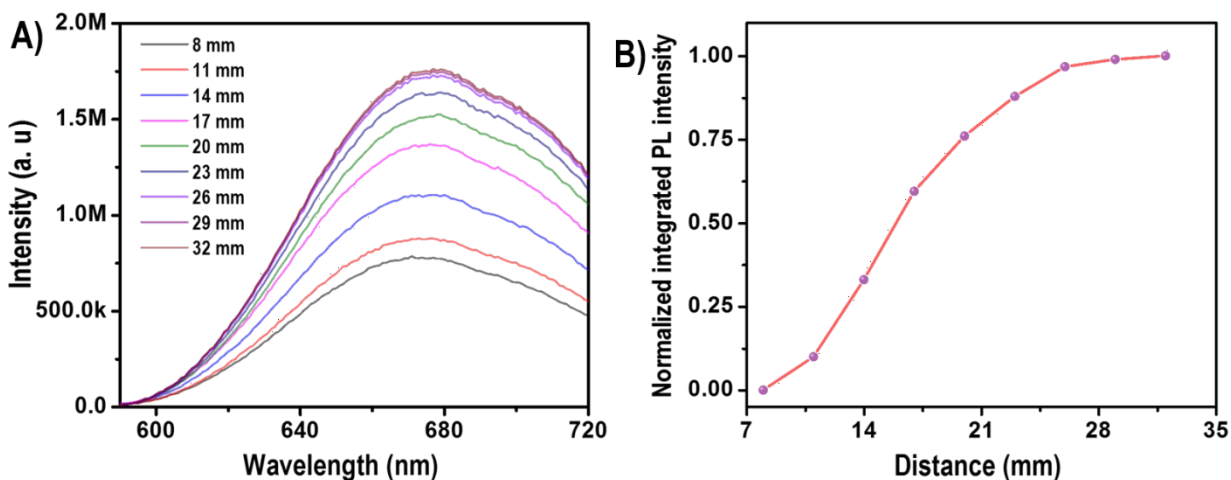


Figure S12. A) Distance-dependent changes in the luminescence intensity of ES Au@BSA measured up to a distance of 32 mm between the tip to the substrate. B) Distance-dependent luminescence of the ES Au@BSA cluster, which show a non-linear increase and indicates the self-quenching of the luminescence in droplets upon increasing the distance.

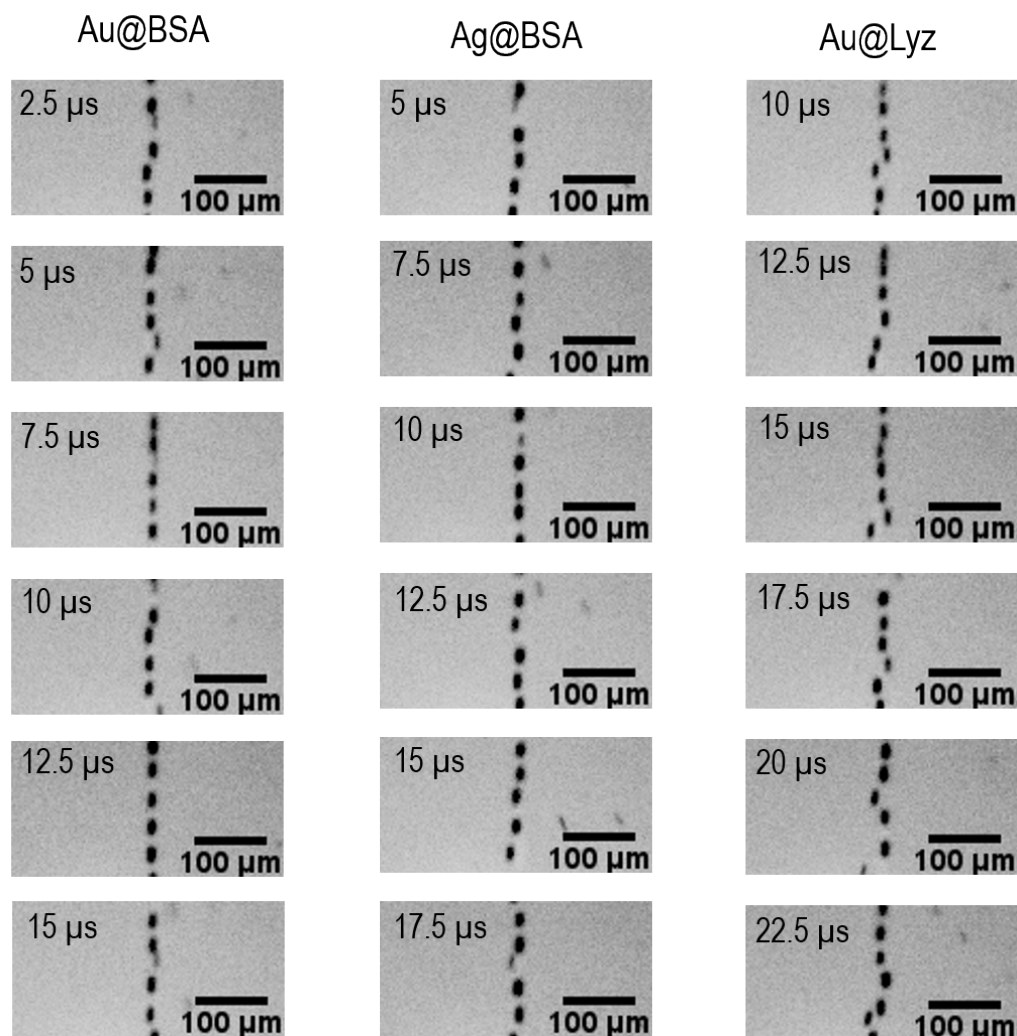


Figure S13. High speed camera images of the individual charged microdroplets (recorded at 400,000 fps) formed as a result of electro spray during the synthesis of Au@BSA, Ag@BSA and Au@Lyz. Movement of these droplets were monitored to calculate the velocity of the droplets.

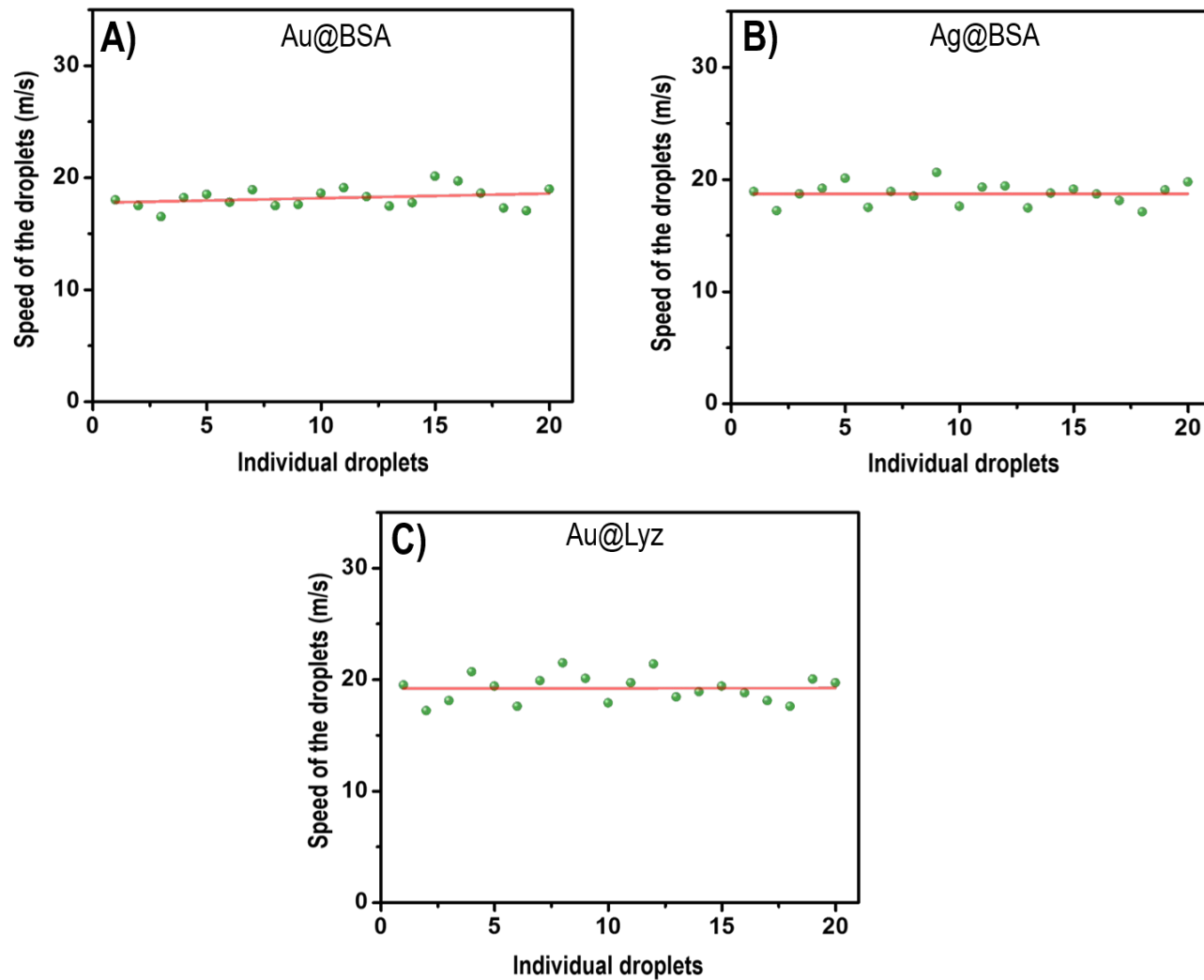


Figure S14. Speed of 20 individual droplets is plotted against droplet number. The velocity distribution is fitted with a straight line and the fitting shows a constant velocity. The calculated speed for A) Au@BSA, B) Ag@BSA and C) Au@Lyz is 17.73 ± 0.41 , 18.69 ± 0.45 and 19.26 ± 0.59 m/s, respectively.

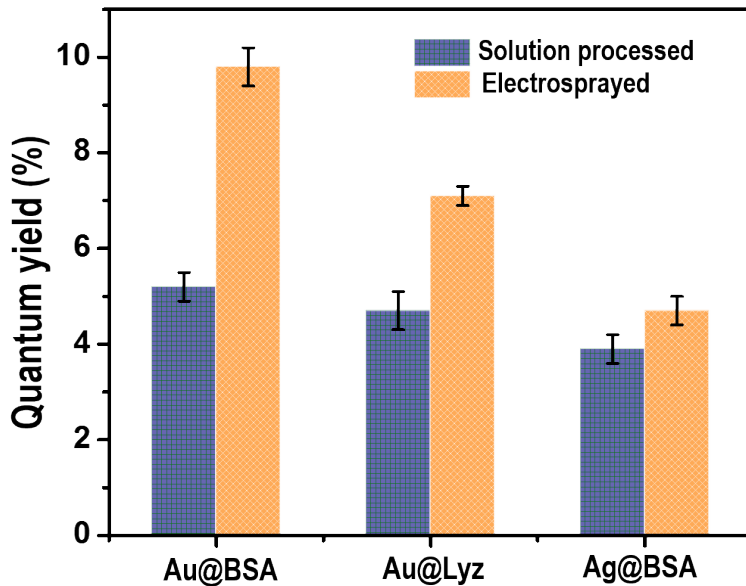


Figure S15. Comparison of the quantum yields of the solution-processed clusters and electrospayed clusters that are prepared under similar concentrations of precursors. Electrospayed clusters have higher QYs than solution-processed clusters which supports luminescence enhancement upon electrospay.

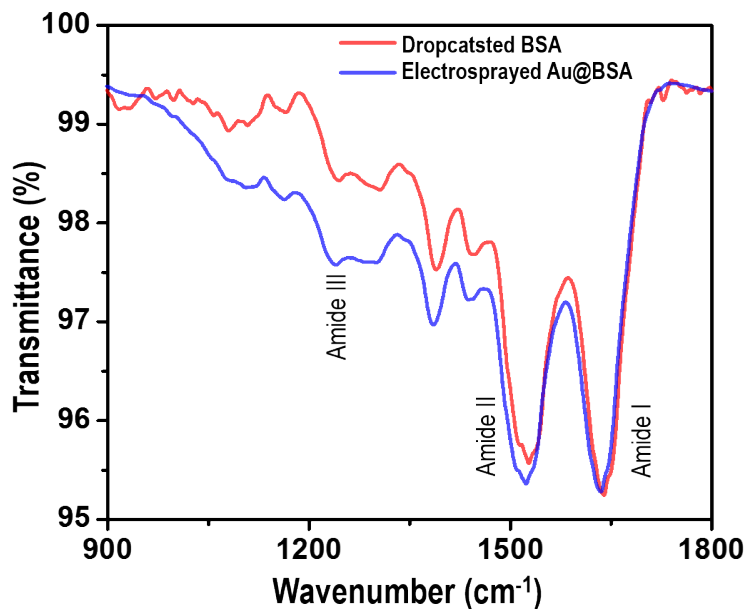


Figure S16. Comparison of the infrared spectra of BSA and ES Au@BSA cluster.

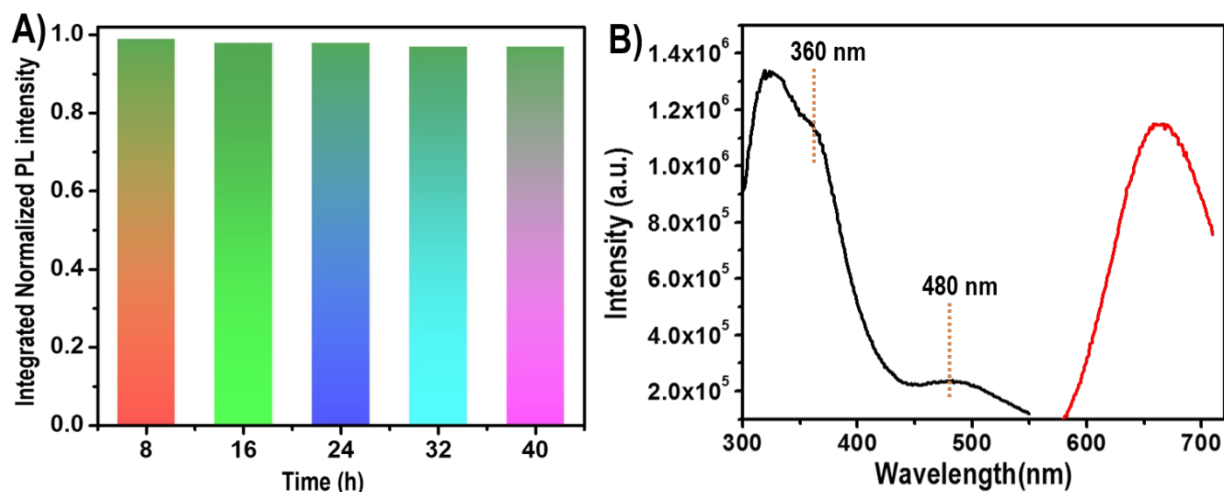


Figure S17. A) Stability of ES Au@BSA in the biological medium, RPMI 1640, was measured. It shows good stability over a period of 40 h and no degradation of the cluster in the medium was noticed. B) Excitation and emission spectra of ES Au@BSA cluster. Excitation spectrum features two peaks at 360 nm and 480 nm. Both the excitations give red luminescence. Excitation at 480 nm was used for the fluorescence imaging of Rb cells.

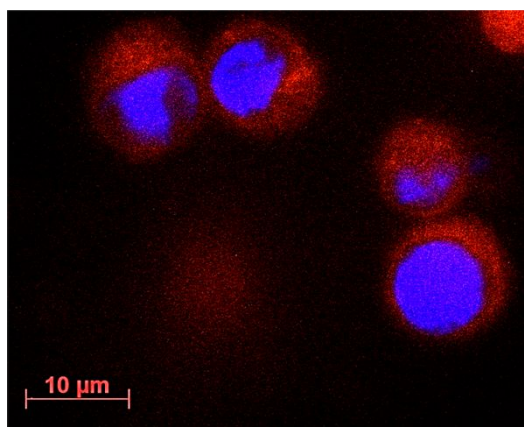


Figure S18. Cellular uptake studies performed on the Rb cells using ES Au@BSA cluster for 1 h. The fluorescence image of the Rb cells show good penetration depth of the clusters into the cell. This suggests that ES Au@BSA could be used for rapid fluorescence imaging of the Rb cells. This

could be used as an alternative to the other luminescent materials which take more time for uptake and causes cell toxicity.

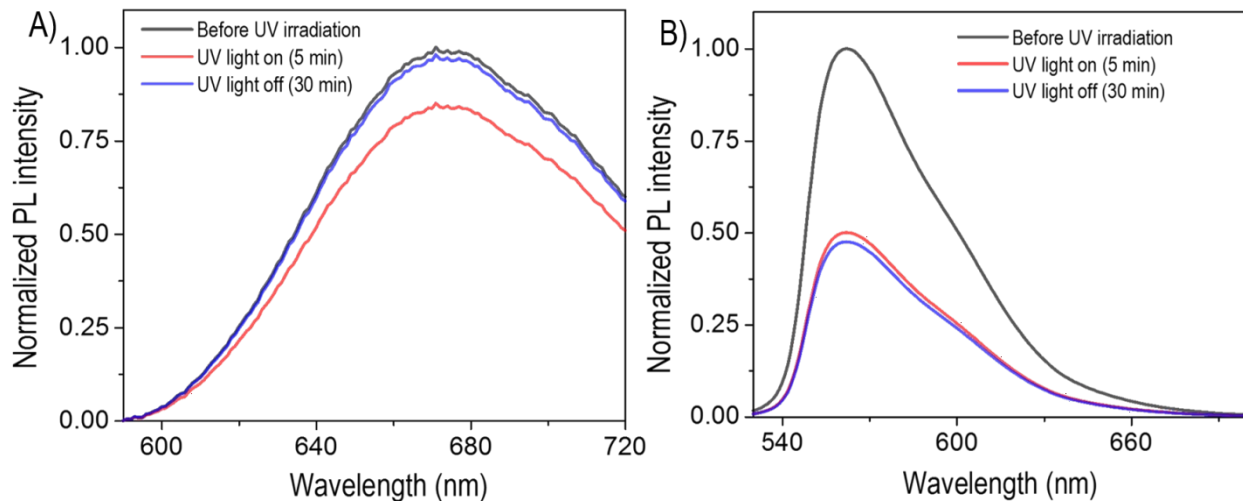


Figure S19. Photo-bleaching experiment performed A) on the ES Au@BSA cluster and B) on the dye (Rhodamine-6G). The dye shows significant degradation as compared to the cluster. Also reversible photo-bleaching was noticed for the cluster which was absent in case of dye (after 30 min in absence of UV light).